Scientific Research Publishing

Advances in Materials Physics and Chemistry, 2017, 7, 353-363
http://www.scirp.org/journal/ampc
ISSN Online: 2162-5328
ISSN Print: 2162-531X

Chemical Durability and Structural Properties of Al_2O_3-CaO-Na_2O-P_2O_5 Glasses Studied by IR Spectroscopy, XRD and SEM

Y. Er-rouissi[1], Z. Chabbou[1], N. Beloued[1], S. Aqdim[1,2*]

[1]Laboratory of Materials Engineering for Environment and Valorization, Hassan II University Ain Chock, Faculty of Sciences, Casablanca, Morocco
[2]Mineral Chemistry Laboratory, Department of Chemistry, Hassan II University Ain Chock, Faculty of Science, Casablanca, Morocco
Email: *said_aq@yahoo.fr

How to cite this paper: Er-rouissi, Y., Chabbou, Z., Beloued, N. and Aqdim, S. (2017) Chemical Durability and Structural Properties of Al_2O_3-CaO-Na_2O-P_2O_5 Glasses Studied by IR Spectroscopy, XRD and SEM. *Advances in Materials Physics and Chemistry*, **7**, 353-363.
https://doi.org/10.4236/ampc.2017.710028

Received: July 7, 2017
Accepted: October 15, 2017
Published: October 18, 2017

Abstract

Various characterization techniques were used to study the composition of the glass series xAl_2O_3-$(40 - x)CaO$-$10Na_2O$-$50P_2O_5$ (with $0 \leq x \leq 10$) in terms of chemical durability, X-ray diffraction, IR spectroscopy and scanning electron microscopy (SEM). The improved chemical durability was attributed to the replacement of easily hydrated P-O-P bonds by covalent and resistant Ca-O-P and Al-O-P bonds. However, the change in the dissolution rate (D_R) versus time showed a marked decrease in chemical durability with increasing the Al_2O_3 content to the detriment of the CaO content. The X-ray diffraction analysis of glasses annealed at 550˚C and 660˚C for 48 hours indicated the presence of pyrophosphate phases and predominant metaphosphates or cyclic metaphosphate phases when the Al_2O_3 content was ≤7.5 mol%. Nevertheless, both, X-ray diffraction and IR spectroscopy confirmed the structural tendency change from metaphosphate (Q^2) and pyrophosphate structural units (Q^1). Toward short isolated orthophosphate units (Q^0) when the Al_2O_3 content above 7.5 mol%. SEM micrographs illustrated that the number of crystallites increased in the glass network when the Al_2O_3 content increased at the expense of the CaO content. An increase in the Al_2O_3 content to 10 mol% led to the formation of a larger number of crystallites of different sizes, dominated by small crystallite sizes assigned to short isolated orthophosphate groups. This phenomenon led to a decrease in chemical durability and seems to be a favorable factor for the formation of the apatite layers which enclose the glass, in a SBF solution test, able of regenerating bone tissue in biomedical application.

Keywords

Bioglasses, Phosphate Glasses, Chemical Durability, XRD, IR, SEM

1. Introduction

Much research has focused on biomedical glasses and glasses as promising materials for diverse applications [1]-[6]. Phosphate glasses have interesting characteristics and properties such as a low melting point, high thermal expansion coefficient, and bioactivity, including the concept of the degradation of biomaterials, which make them useful as biomaterials. Several studies have shown that single phosphate glasses do not have good chemical stability compared to phosphate glasses with several components and have also demonstrated that the macroscopic properties of phosphate bioglasses can be improved, by making small changes in the molar concentration of the modifying oxides and the intermediate network. The latter make it possible to reinforce the structure of the vitreous network while at the same time releasing an amount of calcium and phosphate, during the attack by an SBF solution, necessary to accelerate the regeneration of damaged tissue and improve chemical resistance [7]. Through the use of phosphorus pentoxide **(P_2O_5)** as the initial network, and sodium oxide (Na_2O) with calcium oxide (CaO) as network modifiers, followed by adding other oxides **(Al_2O_3, Fe_2O_3, ZnO and TiO_2)**, the control of degradation may be achieved. Phosphate bioglasses can react with bone tissue through the formation of a hydroxyapatite layer, which is equivalent to the mineral phase of bone; that will then be involved in the process of bone regeneration via a set of physical and chemical reactions [8]. These surface reactions are also responsible for the degradation of the bioglass after implantation [9] [10] [11]. The aim of the present study was to study the structural changes, chemical resistance modification and properties of bioglasses in the **Al_2O_3-CaO-NaO-P_2O_5** system, focusing particularly on the effect of the addition of CaO and **Al_2O_3** to phosphate oxide glasses for use in the medical field. So the study of series of glasses of composition **xAl_2O_3-(40-x)CaO-10NaO-50P_2O_5** (with $0 \leq x \leq 10$ moles%) indicates that the substitution of CaO by Al_2O_3 in the glass network entrained a decrease of the chemical durability, and a important change from metaphosphate (Q^2) and pyrophosphate structural units (Q^1) toward short isolated orthophosphate units (Q^0) when the Al_2O_3 content reached 10 mol%, confirmed by IR spectrum and X-Ray diffraction.

2. Experimental Procedures

Phosphate glasses were produced by the direct melting of a mixture of $(NH_4)_2HPO_4$, $CaCO_3$, Na_2O and Al_2O_3 in suitable proportions. The reagents were ground together and then introduced into a porcelain crucible. Then, they were heated initially to a temperature of 300˚C for 2 hours and then 500˚C for 1 h to

complete decomposition. The reaction mixture was then heated at 900˚C for 40 min and finally at 1080˚C for 30 minutes to obtain a homogeneous liquid. This was then poured onto an aluminum plate which had a temperature of 200˚C to avoid thermal shock. This procedure provided pellets 5 - 10 mm in diameter and 1 to 3 mm thick. The prepared samples were attacked with distilled water at 90˚C for 20 days to determine the dissolution rate estimated from the mass loss. IR spectroscopy analysis was done in a frequency range between 400 cm^{-1} and 1300 cm^{-1} with a resolution of 2 cm^{-1} using a Fourier transform Vertex 70 spectrometer and recorded on a DTGS detector (deuterium triglycine sulfate). The samples were ground and mixed with KBr, which is transparent to infrared. The ratio of the material to KBr in the pellets was 10% to 90% by weight. The analysis by X-ray diffraction was used to identify the structure of the glasses annealed at 550˚C and 660˚C for 48 hours. The samples were analyzed by an X'Pert Pro MPD Panalytical diffractometer. The microstructure of the glass samples was characterized using a scanning electron microscope (SEM).

3. Results

3.1. Ternary Diagram

As can be seen in the ternary diagram in Figure 1, the location of the studied glasses indicates that these glasses are theoretically formed of metaphosphate and pyrophosphate groups. The composition of each sample is given in Table 1.

3.2. Chemical Durability

The dissolution rate (D_R) calculated for the series of bioglasses xAl_2O_3-(40 - x)CaO-10Na_2O-50P_2O_5 (with $0 \le x \le 10$, mol%) is defined as the loss of

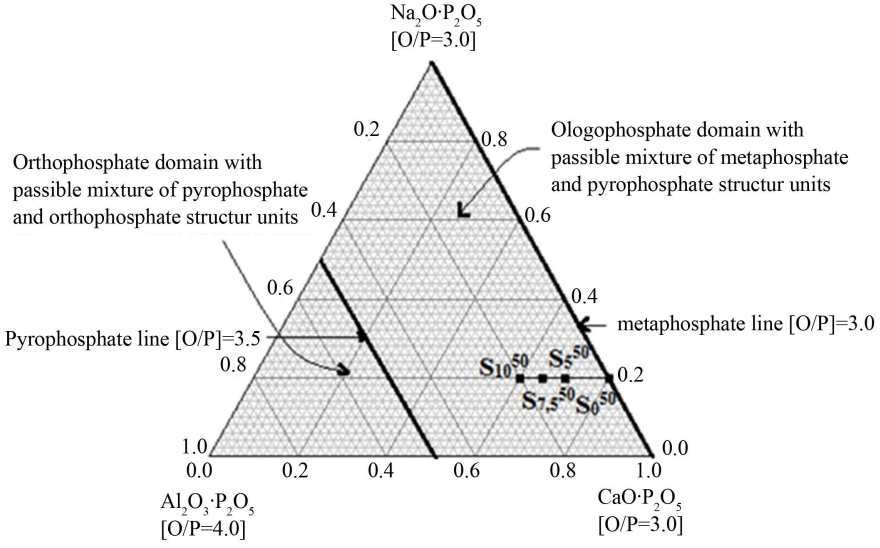

Figure 1. Localization of the studied samples in the ternary diagram of ($Na_2O·P_2O_5$)-($Al_2O_3·P_2O_5$)-($CaO·P_2O_5$). Table 1 gives the corresponding compositions in the quaternary system Al_2O_3-CaO-Na_2O-P_2O_5.

glass mass after immersion in 100 mL of distilled water at 90˚C for 20 days, and expressed as $g{\cdot}cm^{-2}{\cdot}min^{-1}$. The average dissolution rates, which are shown in Figure 2 and Table 2, were measured with respect to the glass surface and the time of exposure. The results show that the chemical durability was improved after increasing the molar percentage of CaO to the detriment of Al_2O_3 [12] [13].

3.3. Infrared Spectra

The IR spectra of the glasses xAl_2O_3-(40 - x)CaO-$10Na_2O$-$50P_2O_5$ (with $0 \le x \le 10$) are shown in Figure 3, and the vibration bands of the assignments are given

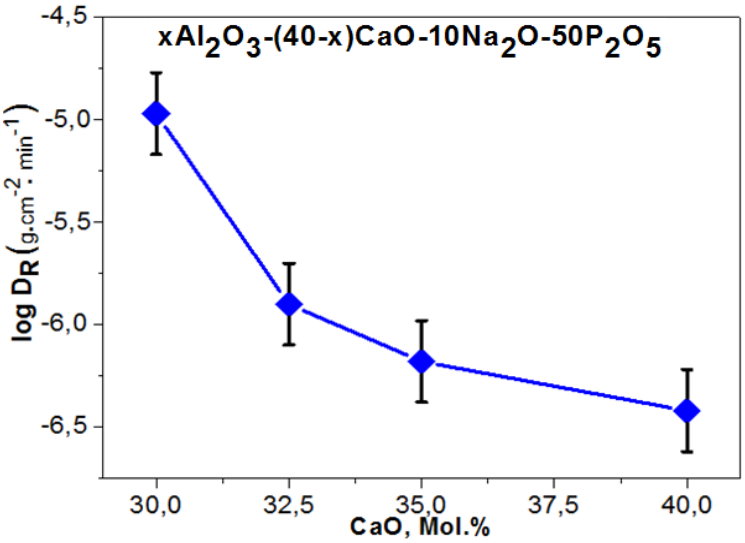

Figure 2. The chemical durability of phosphate glasses versus the Al_2O_3 content.

Table 1. Glass composition expressed in terms of quaternary systems.

Glass sample	Chemical compositions	Glass compositions inside the ternary diagram
S_0^{50}	$10Na_2O{\cdot}40CaO{\cdot}50P_2O_5$	$0.2(Na_2O{\cdot}P_2O_5){\cdot}0.8(CaO{\cdot}P_2O_5)$
S_5^{50}	$10Na_2O{\cdot}35CaO{\cdot}5Al_2O_3{\cdot}50P_2O_5$	$0.2(Na_2O{\cdot}P_2O_5){\cdot}0.1(Al_2O_3{\cdot}P_2O_5){\cdot}0.7(CaO{\cdot}P_2O_5)$
$S_{7.5}^{50}$	$10Na_2O{\cdot}32.5CaO{\cdot}7.5Al_2O_3{\cdot}50P_2O_5$	$0.2(Na_2O{\cdot}P_2O_5){\cdot}0.15(Al_2O_3{\cdot}P_2O_5){\cdot}0.65(CaO{\cdot}P_2O_5)$
S_{10}^{50}	$10Na_2O{\cdot}30CaO{\cdot}10Al_2O_3{\cdot}50P_2O_5$	$0.2(Na_2O{\cdot}P_2O_5){\cdot}0.2(Al_2O_3{\cdot}P_2O_5){\cdot}0.6(CaO{\cdot}P_2O_5)$

Table 2. The composition of the glasses in mol% and some characteristics of the quaternary glasses xAl_2O_3-(40 - x)CaO-$10Na_2O$-$50P_2O_5$.

Glass Sample	The various compositions of glass (mol%)				[O/P]	(Dr) ($g/cm^2/mn$)	Log(Dr)
	P_2O_5	Na_2O	CaO	Al_2O_3	----------	20 days	----------
S_0^{50}	50	10	40	0	3	3.82×10^{-7}	−6.42
S_5^{50}	50	10	35	5	3.1	6.60×10^{-7}	−6.18
$S_{7.5}^{50}$	50	10	32.5	7.5	3.15	1.25×10^{-6}	−5.90
S_{10}^{50}	50	10	30	10	3.2	1.07×10^{-5}	−4.97

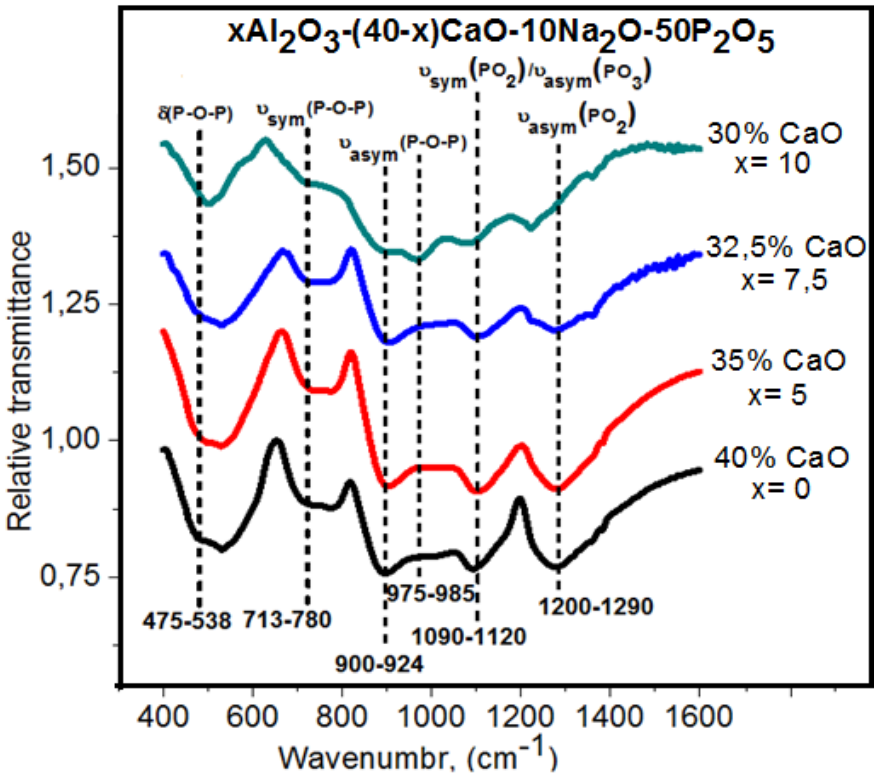

Figure 3. IR spectra of the series of xAl_2O_3-(40 - x)CaO-$10Na_2O$-$50P_2O_5$ glasses, x = 0, 5, 7.5 and 10.

in **Table 3**. All vibration bands are located between 400 and 1300 cm^{-1}. The vibration bands located around 700 - 780 cm^{-1} are attributed to the vibration mode υ_{sym}(P-O-P) of pyrophosphate groups (Q^1), while the bands between 900 - 924 cm^{-1} are attributed to the vibration mode υ_{asym}(P-O-P) of pyrophosphate groups (Q^1). When the Al_2O_3 content reached 10 mol%, we observed the appearance of a band at 980 cm^{-1}, assigned to the vibration mode υ_{asym}(P-O-P) of isolated orthophosphate groups Q^0, to the detriment of bands at 750 - 780 cm^{-1} and 900 - 924 cm^{-1} attributed to pyrophosphate groups, which became single shoulders. The band in the frequency range between 1225 - 1280 cm^{-1} is assigned to the vibration mode $\upsilon_{asym}(PO_2)$ of metaphosphate groups without a bridging oxygen (Q^2) [14] [15] [16], which became weaker when the value of *x* was greater than 7.5 mol%. The vibration bands located around 1070 and 1120 cm^{-1}, characteristic of the vibration modes $\upsilon_{ym}(PO_2)$ and $\upsilon_{asym}(PO_3)$ of tetrahedral units, $Q^2 + Q^1$, which are a mixture of pyrophosphate and metaphosphate groups, also underwent a decrease in intensity when the Al_2O_3 content exceeded 5 mol%.

3.4. X-Ray Diffraction

X-ray diffraction confirmed the vitreous character of all the samples. The XRD spectra of samples $\mathbf{S_0^{50}}$ to $\mathbf{S_{10}^{50}}$, annealed at 550˚C and 660˚C for 48 h are shown in **Figure 4**. Several phases were detected, including calcium metaphosphate or

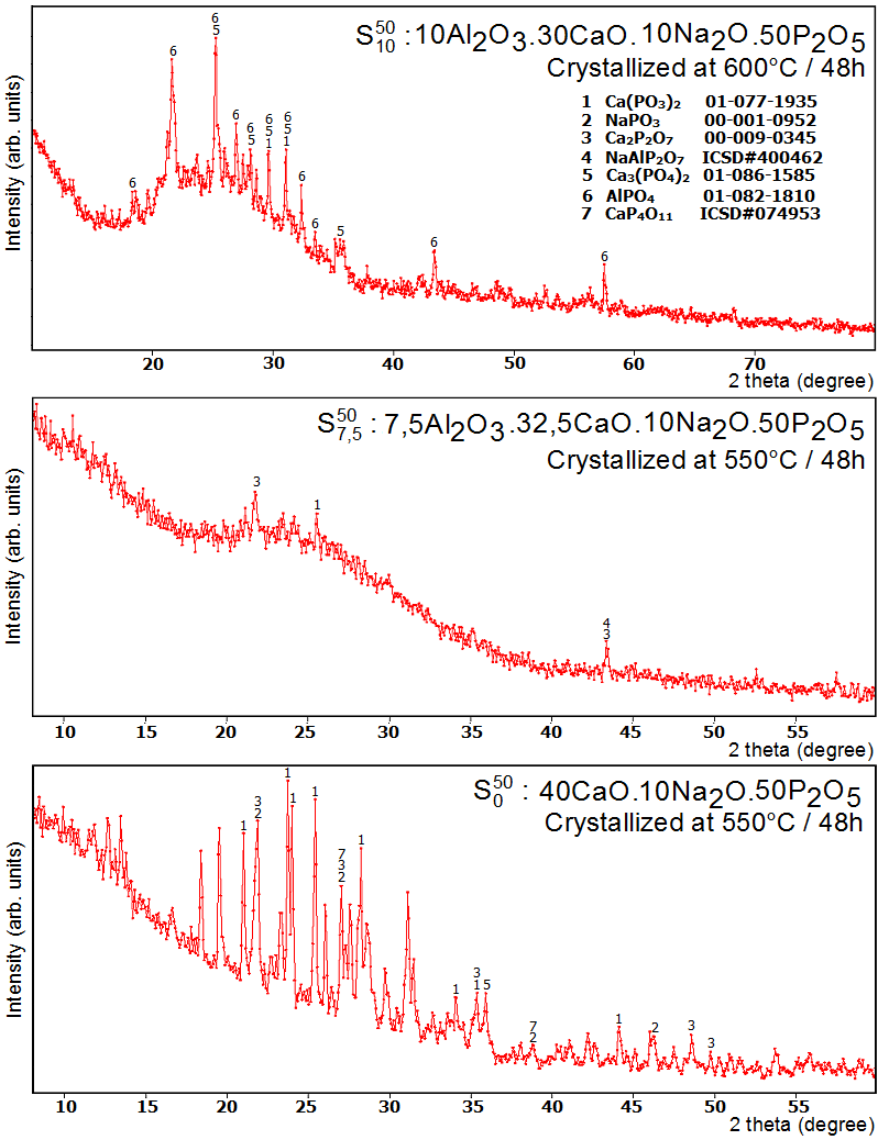

Figure 4. XRD patterns for the glass samples S_0^{50}, $S_{7.5}^{50}$ and S_{10}^{50} after heat treatment for 48 h in an air atmosphere at 550˚C and 600˚C.

cyclic metaphosphate ($Ca(PO_3)_2$, $NaPO_3$ and $Ca_2P_4O_{11}$ in sample S_0^{50}, while the same figure shows calcium pyrophosphate ($Ca_2P_2O_7$), sodium-aluminum pyrophosphate ($NaAlP_2O_7$) and $Ca(PO_3)_2$ in sample $S_{7.5}^{50}$ [12] [13] [14] [15] [17]. However, for the compound S_{10}^{50}, there is a radical structural change which indicates the predominance of orthophosphates phase type $AlPO_4$ and eventually $Ca_3(PO_4)_2$.

3.5. Scanning Electron Microscopy

Figure 5 shows SEM micrographs of sample $\mathbf{S_0^{50}}$ with the compositions $40CaO{\cdot}10Na_2O{\cdot}50P_2O_5$ (**Figure 5(a)**), as well as samples $\mathbf{S_{7.5}^{50}}$ and $\mathbf{S_{10}^{50}}$ with the compositions $7.5Al_2O_3{\cdot}32.5CaO{\cdot}10Na_2O{\cdot}50P_2O_5$ (**Figure 5(b)**) and $10Al_2O_3{\cdot}30CaO{\cdot}10Na_2O{\cdot}50P_2O_5$ (**Figure 5(c)**), respectively. The SEM micro graph in

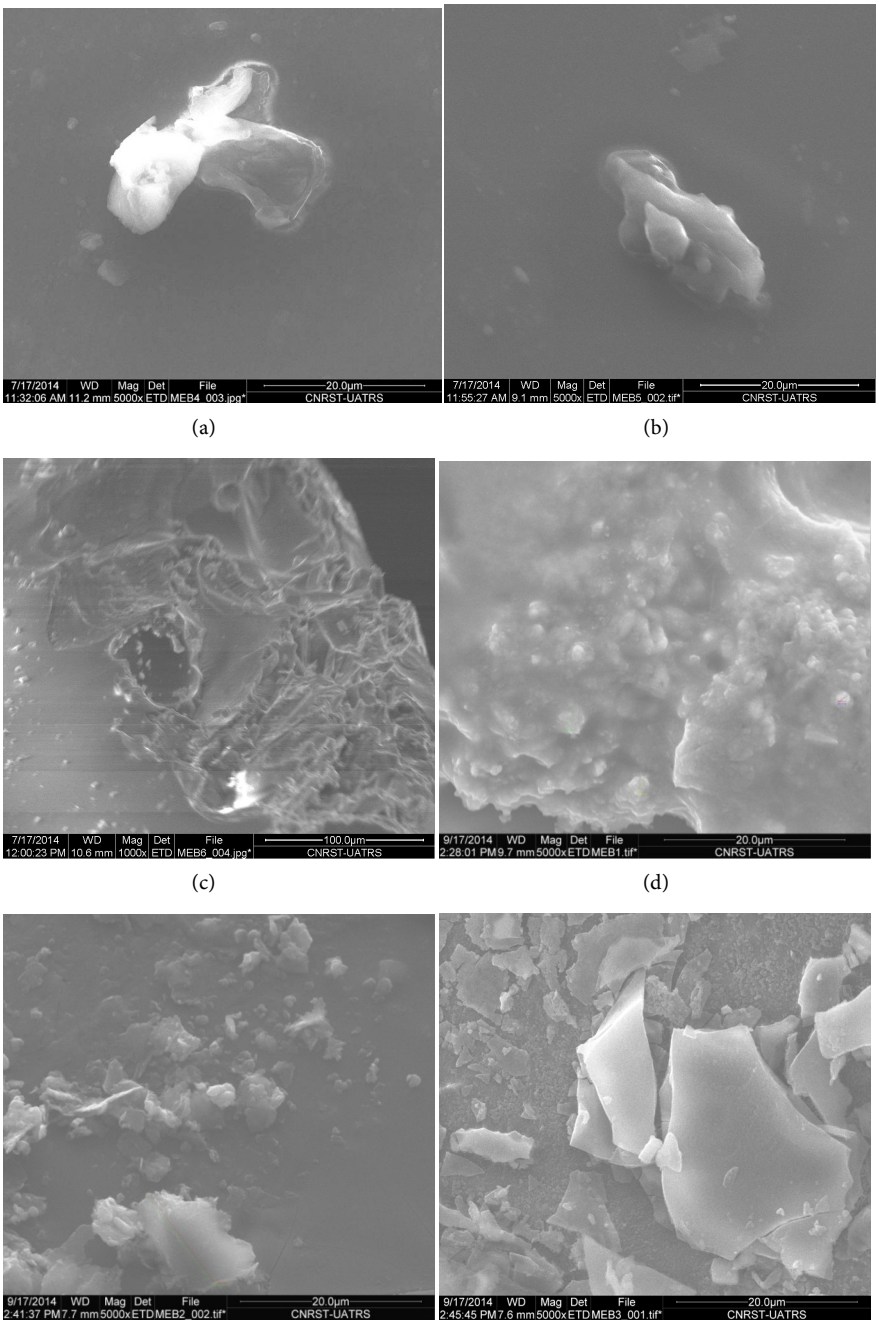

Figure 5. SEM micrograph showing the visual structure of the samples S_0^{50} (a); $S_{7.5}^{50}$ (b) and S_{10}^{50}**(c)** before attack and of the samples S_0^{50} (d); $S_{7.5}^{50}$ (e) and S_{10}^{50} (f) after attack in distillated water at 90˚C for 20 days.

Figure 5 illustrates the morphology of the glasses, before and after immersion in distillated water for 20 consecutive days, considered in this work. It shows the existence of two phases, one crystalline and the other glass [13] [16] [18] [19]. It also indicates the formation of agglomerates of the crystalline phase from one micrometer to a few tens of micrometers in size. The SEM micrograph also indicates that the number of crystallites increased from S_0^{50} to S_{10}^{50} when the Al_2O_3

Table 3. The assignments of different vibration bands of the IR spectra of the quaternary xAl_2O_3-(40-x)CaO-10NaO-$50P_2O_5$.

Frequency regions (cm^{-1})	Assignments	Ref.
440 - 560	Vibration mode δ_{ske}(P-O-P)	[17] [18]
700 - 780	Vibration mode υ_{Sym}(P-O-P) in unit Q^1	[19]
900 - 940	Vibration mode υ_{Asym}(P-O-P) in unit Q^1	[19]
980 - 1020	Vibration mode υ_{Asym}(P-O-P) in unit Q^0	[18]
1070 - 1120	Vibration mode $\upsilon_{sym}(PO_2)/\upsilon_{Asym}(PO_3)$ in units $Q^1 + Q^2$	[17]
1200 - 1290	Vibration mode $\upsilon_{Asym}(PO_2)$ in unit Q^2	[17] [18]

content increased at the expense of the CaO content.

4. Discussion

In this study, we prepared a glass series with different percentages of phosphate oxides; Al_2O_3, Na_2O, CaO and P_2O_5 were used as the basic constituents. In this series, we substituted the CaO oxide with Al_2O_3 oxide while keeping the percentage of P_2O_5 and Na_2O oxides constant. The improved chemical durability was attributed to the replacement of the easily hydrated P-O-P bonds by covalent and resistant Ca-O-P bonds. However, the substitution of CaO with Al_2O_3 in the glass network led to a considerable decrease in chemical durability. The IR spectra indicated a radical structural change from metaphosphate or cyclic metaphosphate and pyrophosphate towards short majority isolated orthophosphate groups when the Al_2O_3 content was above 7.5 mol%. Also, the structure deduced from the vibrational spectroscopy is compatible with the localizations of the analysed compounds $\mathbf{S_0^{50}}$ to $\mathbf{S_{7.5}^{50}}$ inside the ternary diagram given in **Figure 1** with the exception of compound $\mathbf{S_{10}^{50}}$ which predominantly contains isolated orthophosphate groups This is seems to due to the physical and chemical properties of the intermediate oxide that participates in the glass formation (melting temperature, rate of Ca + Al/P.) [19] [20] [21]. The X-ray diffraction spectra confirmed the presence of $Ca_2(P_2O_7)$, CaP_4O_{11}, $Ca(PO_3)_2$ and $Ca_3(PO_4)_2$ crystalline phases in the $\mathbf{S_0^{50}}$ sample and $NaAl(P_2O_7)$, $Ca_2(P_2O_7)$ and $Ca(PO_3)_2$ crystalline phases in the $\mathbf{S_{7.5}^{50}}$ sample, while in the S_{10}^{50} sample, the structure obtained is formed of almost crystalline isolated orthophosphate phase $AlPO_4$ with some trace of $Ca_3(PO_4)_2$. The SEM micrographs (**Figure 5**) indicated that the number of crystallites increased from $\mathbf{S_0^{50}}$ to $\mathbf{S_{10}^{50}}$ when the Al_2O_3 content increased at the expense of the CaO content. The increase in crystallites in phosphate network glasses, in general, improves the chemical durability [16] [18]. In our case, we observed the opposite. It was also noted in these micrographs that crystallite metaphosphate cyclic chains predominated in $\mathbf{S_0^{50}}$, to different sizes of crystallites observed in $\mathbf{S_{7.5}^{50}}$ and finally to a larger number of crystallites of different sizes in $\mathbf{S_{10}^{50}}$, likely dominated by small crystallite sizes assigned to isolated orthophosphate groups. The increase in short chain isolated orthophosphate

groups in the glass network at the expense of cyclical chain metaphosphate groups and pyrophosphate chains when the Al_2O_3 content exceeded 7.5 mol% can be explained by the fact that we were close to the border area between crystal and glass. The number of crystallites of different sizes generally increased and exceeded the equilibrium that must be established between the glass and the crystallites, which led to a significant decrease in chemical durability [19]. Indeed the compound $\mathbf{S_{10}^{50}}$, has an opaque white appearance which explains its frontal position between the glass and the crystal. However, the favorable formation of the isolated orthophosphate groups when the CaO oxide is substituted by Al_2O_3 oxide, and especially when the Al_2O_3 level reaches 10 mol%, can be of great utility in the formation of the apatite layers in an organic-substance-free a cellular simulated body fluid (SBF), able of regenerating bone.

5. Conclusion

The structure and chemical durability of a glass series composed of xAl_2O_3-(40 – x)CaO-10Na_2O-50P_2O_5 (with $0 \leq x \leq 10$) (mol%) were investigated using various techniques such as IR, X-ray diffraction and SEM. The improved chemical durability in these glasses was attributed to the replacement of the easily hydrated P-O-P bonds by covalent and resistant Ca-O-P bands. However, the substitution of CaO by Al_2O_3 in the glass network led to a considerable decrease in the chemical durability. The IR spectra indicated a radical structure change from metaphosphate or cyclic metaphosphate and pyrophosphate towards short isolated orthophosphate groups when the Al_2O_3 content was above 7.5 mol%. Consequently, we can predict the depolymerization of the large phosphate network into isolated short chains of the orthophosphate (Q°) type. The SEM micrographs of $\mathbf{S_0^{50}}$, $\mathbf{S_{7.5}^{50}}$ and $\mathbf{S_{10}^{50}}$ illustrate that the number of crystallites increased from $\mathbf{S_0^{50}}$ to $\mathbf{S_{10}^{50}}$ when the Al_2O_3 content increased at the expense of the CaO content. The increase in the number of crystallites that led to the formation of isolated short chains of the orthophosphate (Q°) type almost certainly caused disproportionality between the glass and the crystallites, which caused a significant decrease in chemical durability. Hence, a better understanding of glass corrosion is very relevant to the industry in the development of technical bioglasses to achieve both good performance and, at the same time, provide calcium ion and Orthophosphate ions, in an aqueous solution or SBF solution, necessary for the formation of effective hydroxyapatite layers in bone regeneration in biomedical applications.

Acknowledgements

The authors wish to thank National Center for Scientific and Technical Research [Division of Technical Support Unit for Scientific Research (TSUSR) Rabat, Morocco] for their assistance to the realization of this work. We also thank Pr. R. Elouatib (Laboratory physic and chemistry of inorganic materials) for the support that has brought us.

References

[1] Velli, L.L., Varsamis, C.P.E., Kamitsos, E.I., Möncke, D. and Ehrt, D. (2005) Structural Investigation of Metaphosphate Glasses. *Physics and Chemistry of Glasses-European Journal of Glass Science and Technology Part B*, **46**, 178-181.

[2] Kiani, A., Hanna, J.V., King, S.P., Rees, G.J., Smith, M.E., Roohpour, N., Knowles, J.C. (2012) Structural Characterization and Physical Properties of P_2O_5-CaO-Na_2O-TiO_2 Glasses by Fourier Transform Infrared, Raman and Solid-State Magicangle Spinning Nuclear Magnetic Resonance Spectroscopies. *Acta Biomaterialia*, **8**, 333-340. https://doi.org/10.1016/j.actbio.2011.08.025

[3] Brow, R.K., ClickC, A. and Alam T.M. (2000) Modifier Coordination and Phosphate Glass Networks. *Journal of Non-Crystalline Solids*, **274**, 9-16. https://doi.org/10.1016/S0022-3093(00)00178-2

[4] Moss, R.M., Neel, E.A.A., Pickup, D.M., Twyman, H.L., Martin, R.A., Henson, M.D. and Newport, R.J. (2010) The Effect of Zinc and Titanium on the Structure of Calcium-Sodium Phosphate Based Glass. *Journal of Non-Crystalline Solids*, **356**, 1319-1324. https://doi.org/10.1016/j.jnoncrysol.2010.03.006

[5] Colak, S.C. and Aral, E. (2011) Optical and Thermal Properties of P_2O_5-Na_2O-CaO-Al_2O_3: CoO Glasses Doped with Transition Metals. *Journal of Alloys and Compounds*, **509**, 4935-4939. https://doi.org/10.1016/j.jallcom.2011.01.172

[6] Ahmed, I., Lewis, M.P., Nazhat, S.N. and Knowles, J.C. (2005) Quantification of Anion and Cation Release from a Range of Ternary Phosphate-Based Glasses with Fixed 45 mol% P_2O_5. *Journal of Biomaterial Applications*, **20**, 65-80. https://doi.org/10.1177/0885328205049396

[7] Rajendran, V., GayathriDevi, A.V., Azooz, M. and El-Batal, F.H. (2007) Physicochemical Studies of Phosphate Based P_2O_5-Na_2O-CaO-TiO_2 Glasses for Biomedical Applications. *Journal of Non-Crystalline Solids*, **353**, 77-84. https://doi.org/10.1016/j.jnoncrysol.2006.08.047

[8] Weiss, D.S.L., Torres, R.D., Buchner, S., Blunk, S. and Soares, P. (2014) Effect of Ti and Mg Dopants on the Mechanical Properties, Solubility, and Bioactivity *in vitro* of a Sr-Containing Phosphate Based Glass. *Journal of Non-Crystalline Solids*, **386**, 34-38. https://doi.org/10.1016/j.jnoncrysol.2013.11.036

[9] lewinski, M., Schickle, K., Lindner, M., Kirsten, A., Weber, M. and Fischer, H. (2013) The Effect of Crystallization of Bioactive Bioglass 45S5 on Apatite Formationnd Degradation. *Dental Materials*, **29**, 1256-1264. https://doi.org/10.1016/j.dental.2013.09.016

[10] Balamurugan, A., Balossier, G., Kannan, S., Michel, J., Rebelo, A.H. and Ferreira, J.M. (2007) Development and *in vitro* Characterization of Sol-Gel Derived CaO-P_2O_5-SiO_2-ZnO Bioglass. *Acta Biomaterialia*, **3**, 255-262. https://doi.org/10.1016/j.actbio.2006.09.005

[11] Barrios de Arenas, I., Schattner, C. and Vásquez, M. (2006) Bioactivity and Mechani Cal Properties of Na_2O-CaO-SiO_2-P_2O_5 Modified Glasses. *Ceramics International*, **32**, 515-520.

[12] Bengisu, M., Brow, R.K., Yilmaz, E., Moguš-Milanković, A. and Reis, S.T. (2006) Aluminoborate and Aluminoborosilicate Glasses with High Chemical Durability and the Effect of P_2O_5 Additions on the Properties. *Journal of Non-Crystalline Solids*, **352**, 3668-3676.

[13] Chabbou, Z. and Aqdim, S. (2014) Chemical Durability and Structural Proprieties of the Vitreous Part of the System xCaO-(40−x)ZnO-15Na_2O-45P_2O_5. *Advances in*

Materials Physics and Chemistry, **4**, 179. https://doi.org/10.4236/ampc.2014.410021

[14] Cai, S., Zhang, W.J., Xu, G.H., Li, J.Y., Wang, D.M. and Jiang, W. (2009) Microstructural Characteristics and Crystallisation of CaO-P_2O_5-Na_2O-ZnO Glass Ceramics Prepared by the Sol-Gel Method. *Journal of Non-Crystalline Solids*, **355**, 273-279.

[15] Aqdim, S., Sayouty, E.H. and Elouadi, B. (2008) Structural and Durability Investigation of the Vitreous Part of the System $(35-z)Na_2O$-zFe_2O_3-$5Al_2O_3$-$60P_2O_5$. *Eurasian Chemico-Technological Journal*, **10**, 9-17.

[16] Aqdim, S. and Ouchetto, M. (2013) Elaboration and Structural Investigation of Iron (III) Phosphate Glasses. *Advances in Materials Physics and Chemistry*, **3**, 332-339. https://doi.org/10.4236/ampc.2013.38046

[17] Sun, H.T., Zhou, J. and Qiu, J. (2014) Recent Advances in Bismuth Activated Photonic Materials. *Progress in Materials Science*, **64**, 1-72.

[18] Aqdim, S. and Albizane, A. (2015) Structural Feature and Chemical Durability of So dium Aluminium Iron Phosphate Glasses. *Journal of Environmental Science, Computer Science and Engineering & Technology*, **4**, 509-521.

[19] Beloued, N. and Aqdim, S. (2016) Correlation between Chemical Durability Behavior and Structural Approach of the Vitreous Part of the System $55P_2O_5$-$2Cr_2O_3$ $43-x)Na_2O$-$xPbO$. *Advances in Materials Physics and Chemistry*, **6**, 149-156

[20] Ouchetto, M. (1993) Caractérisation et Approche structural de la région vitreuse du système ternaire Li_2O-CdO-P_2O_5 Diplôme d'étude de $3^{ème}$ Cycle Sciences Phy siques. Faculty of Sciences Rabat, University Mohammed V, Morocco.

[21] Aqdim, S. (1990) Identification et étude thermique et électrique des phasesvi treuses des systèmes ternaires Li2O-M2O3-P2O5 (M = Cr, Fe) Diplôme D'étude Supérieure de 3ème Cycle de Spécialité. Faculty of Sciences Rabat. University Mo hammed V, Morocco.